

# Rank-1 accelerated illumination recovery in scanning diffractive imaging by transparency estimation.

Stefano Marchesini

*Advanced Light Source, Lawrence Berkeley National Laboratory, Berkeley, CA 94720 (USA)*

Hau-tieng Wu

*Department of Mathematics, University of Toronto, Toronto, Ontario (CANADA)*

Illumination retrieval in scanning diffractive imaging a.k.a. ptychography is challenging when the specimen is weakly scattering or surrounded by empty space. We describe a rank-1 acceleration method for weakly scattering or piecewise smooth specimens.

Ptychography is an increasingly popular technique to achieve diffraction limited imaging over a large field of view without the need for high quality optics<sup>2-5,7,10-16,20,22,23,25-29,31,32,35,37</sup>. Since the reconstruction of ptychographic data is a non-linear problem, there are still many open problems<sup>19</sup>, nevertheless the phase retrieval problem is made tractable by recording multiple diffraction patterns from the same region of the object, compensating phase-less information with a redundant set of measurements. Data redundancy enables to handle experimental uncertainties as well. Methods to work with unknown illuminations or “lens” were proposed<sup>4,23,27,28</sup>. They are now used to calibrate high quality x-ray optics<sup>10,12,15</sup>, x-ray lasers<sup>24</sup> and space telescopes<sup>21</sup>. More recently, position errors<sup>3,8,16</sup>, background<sup>9,30</sup>, noise statistics<sup>7,29</sup> and partially coherent illumination<sup>1,6,14,34</sup>. Situations when sample, illumination function, incoherent multiplexing effects, as well as positions, vibrations, binning, multiplexing, fluctuating background are unknown parameters in high dimensions have been added to the nonlinear optimization to fit the data using projections, gradient, augmented lagrangian<sup>33</sup>, conjugate gradient, Newton<sup>36</sup>, and spectral methods<sup>2,18,19</sup>. Here we focus on the illumination retrieval problem. We utilize the notation described in<sup>18,19</sup>, which is summarized below.

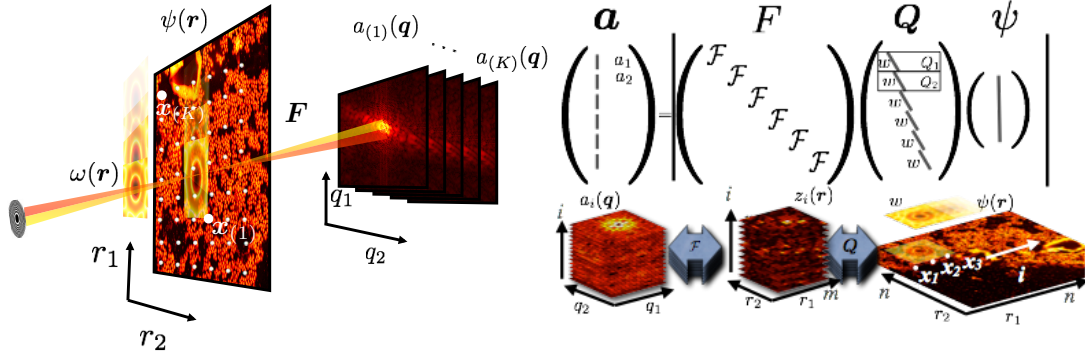


FIG. 1. The measured amplitudes  $\mathbf{a}$  and the relationship with an unknown object  $\psi$  in standard “Far Field” ptychography. Geometric representation of the operators involved in simulating a ptychographic imaging experiment<sup>18,19</sup>.

## I. BACKGROUND

The relationship between an unknown discretized object  $\psi$ , and the diffraction measurements  $\mathbf{a}_{(i)}$  collected in a ptychography experiment (see figure 1) can be represented compactly as:

$$\mathbf{a} = |\mathbf{FQ}\psi^V|, \text{ or } \begin{cases} \mathbf{a} = |\mathbf{Fz}|, \\ \mathbf{z} = \mathbf{Q}\psi^V, \end{cases} \quad (1)$$

where  $\psi^\vee$  is the object  $\psi$  in vector form. Eq. (1) can be expressed as:

$$\begin{aligned} \begin{bmatrix} \mathbf{a}_{(1)} \\ \vdots \\ \mathbf{a}_{(K)} \end{bmatrix} &= \begin{bmatrix} \mathbf{F} \in \mathbb{C}^{Km^2 \times Km^2} & \mathbf{z} \in \mathbb{C}^{Km^2} \\ \begin{bmatrix} F & \dots & 0 \\ \vdots & \ddots & \vdots \\ 0 & \dots & F \end{bmatrix} & \begin{bmatrix} \mathbf{z}_{(1)} \\ \vdots \\ \mathbf{z}_{(K)} \end{bmatrix} \end{bmatrix}, \quad \begin{bmatrix} \mathbf{z}_{(1)} \\ \vdots \\ \mathbf{z}_{(K)} \end{bmatrix} = \begin{bmatrix} \mathbf{Q} \in \mathbb{C}^{Km^2 \times n^2} & \psi \in \mathbb{C}^{n^2} \\ \begin{bmatrix} \text{diag}(w) \mathbf{T}_{(1)} \\ \vdots \\ \text{diag}(w) \mathbf{T}_{(K)} \end{bmatrix} & \begin{bmatrix} \psi_1 \\ \vdots \\ \psi_{n^2} \end{bmatrix} \end{bmatrix}, \end{aligned}$$

where  $\mathbf{z}$  are  $K$  frames extracted from the object  $\psi$  and multiplied by the illumination function  $w$ ,  $\mathbf{F}$  is the associated 2D DFT matrix when we write everything in the stacked form, that is,  $F$  is a  $m^2 \times m^2$  matrix satisfying  $F_{lk} = \mathbf{e}_l^T F \mathbf{e}_k = e^{iq_m^{-1}(l-1) \cdot r_m^{-1}(k-1)}$ . For experimental geometries related to what has been described above, such as Near Field, ‘‘Fresnel’’, Fourier ptychography, through-focus<sup>5,26,31,32</sup> one can substitute the simple Fourier transform with the appropriate propagator.

The illumination matrix  $\mathbf{Q}$  encodes information about illumination  $w \in \mathbb{C}^{m^2}$ , and the  $K$  relative translations between the probe  $w$  and the object  $\psi$ . In particular, the  $(i)$  block denoted as  $\mathbf{Q}_{(i)} \in \mathbb{C}^{m^2 \times n^2}$  extracts one frame from the object and multiplies by the illumination  $w$ :

$$\mathbf{Q}_{(i)} = \text{diag}(w^\vee) \mathbf{T}_{(i)} \in \mathbb{C}^{m^2 \times n^2}, \quad \mathbf{Q} = \begin{pmatrix} \text{diag}(w^\vee) \mathbf{T}_{(1)} \\ \text{diag}(w^\vee) \mathbf{T}_{(2)} \\ \vdots \\ \text{diag}(w^\vee) \mathbf{T}_{(K)} \end{pmatrix}, \quad (2)$$

where the matrix  $\mathbf{T}_{(i)}$  extract an  $m \times m$  frame out of an  $n \times n$  image. The matrix  $T_{(i)}$  can be expressed in terms of a translation matrix  $\mathbf{C}_x$  which circularly translates by  $\mathbf{x}$  in  $D^{n \times n}$  and the *restriction matrix*  $\mathbf{R}$ , which is of size  $m^2 \times n^2$  so that  $\mathbf{R}(i, i) = 1$  for all  $i = 1, \dots, m^2$  and 0 otherwise:

$$\mathbf{T}_{(i)} = \mathbf{R} \mathbf{C}_{\mathbf{x}(i)}, \quad \mathbf{T} = \begin{pmatrix} \mathbf{T}_{(1)} \\ \mathbf{T}_{(2)} \\ \vdots \\ \mathbf{T}_{(K)} \end{pmatrix}. \quad (3)$$

In the following, to simplify the notation, we will not distinguish between  $w$  (resp.  $\psi$ ) and its vector form  $w^\vee$  (resp.  $\psi^\vee$ ) and use the same notation  $w$  (resp.  $\psi$ ). We simplify Eq (2) as

$$\mathbf{Q} = \text{diag}(\mathbf{S}w) \mathbf{T}, \quad (4)$$

where we define  $\mathbf{S} \in \mathbb{R}^{Km^2 \times m^2}$  to be the matrix that replicates the illumination probe  $w$  into  $k$  stack of frames, that is,  $\mathbf{S}$  is a  $K \times 1$  block matrix with the  $m^2 \times m^2$  identity matrix as the block. There is a relationship between  $\psi, w$  and  $\mathbf{z}$ :

$$\mathbf{z} = \mathbf{Q}\psi = \text{diag}(\mathbf{S}w) \mathbf{T}\psi = \text{diag}(\mathbf{T}\psi) \mathbf{S}w \quad (5)$$

due to the fact that  $\text{diag}(\mathbf{S}w) \mathbf{T}\psi$  is the entry-wise product of  $\mathbf{S}w$  and  $\mathbf{T}\psi$ .

In the notation used in this paper, projection operators are expressed as:

$$P_{\mathbf{Q}} = \mathbf{Q}(\mathbf{Q}^* \mathbf{Q})^{-1} \mathbf{Q}^*$$

$$P_{\mathbf{a}} = \mathbf{F}^* \frac{\mathbf{F} \mathbf{z}}{|\mathbf{F} \mathbf{z}|} \mathbf{a}.$$

## II. ALTERNATING PROJECTIONS PROBE, FRAMES, IMAGE

The standard update<sup>23,27</sup> proceeds in three steps updating the estimate of the illumination  $w$ , estimate of the specimen  $\psi$ , and the frames  $\mathbf{z}$  based on experimental geometry and data. First update the image  $\psi$  by (5):

$$\psi \leftarrow (\mathbf{Q}^* \mathbf{Q})^{-1} \mathbf{Q}^* \mathbf{z} = \frac{\mathbf{T}^* \text{diag}(\mathbf{S} \bar{w}) \mathbf{z}}{\mathbf{T}^* (\mathbf{S} |w|^2)}, \quad (6)$$

where the second equality holds due to (4); that is,  $\mathbf{Q}^*\mathbf{Q} = \text{diag}(\mathbf{T}^*(\mathbf{S}|w|^2))$ . Note that for the sake of simplifying notation, we represent  $\text{diag}(v)^{-1}B =: \frac{B}{v}$  when  $\text{diag}(v)$  is invertible diagonal matrix. Second, by (5), update the probe  $w$ :

$$w \leftarrow \frac{\mathbf{S}^* \text{diag}(\mathbf{T}\bar{\psi})\mathbf{z}}{\mathbf{S}^*\mathbf{T}|\psi|^2}, \quad (7)$$

Third update the frames using the new probe embedded in  $\mathbf{Q}$ , and the  $P_{\mathbf{a}}$  operator:

$$\mathbf{z} \leftarrow P_{\mathbf{a}} \text{diag}(\mathbf{S}w)\mathbf{T}\psi. \quad (8)$$

Note that Equation (7) is motivated by (5). In fact, we have  $\text{diag}(\mathbf{T}\bar{\psi})\mathbf{z} = \text{diag}(|\mathbf{T}\psi|^2)\mathbf{S}w$ . And note that by a direct calculation,  $\mathbf{S}^* \text{diag}(|\mathbf{T}\psi|^2)\mathbf{S} = \text{diag}(\sum_i \mathbf{T}_{(i)}|\psi|^2)$ , which leads to (7) when all entries of  $\mathbf{S}^*\mathbf{T}|\psi|^2$  are not zero. When there is zero entry in  $\mathbf{S}^*\mathbf{T}|\psi|^2$ , we may consider  $\max\{\mathbf{S}^*\mathbf{T}|\psi|^2, \epsilon\}$ , where  $\epsilon > 0$  is a small positive number determined by the user. Note that  $\mathbf{S}^*$  plays the role of averaging.

### III. THE RELATIONSHIP BETWEEN PROBES (ILLUMINATION) AND FRAMES

We now analyze here the symmetry between  $\mathbf{Q}$  and  $\mathbf{z}$ , that is, we look at the frame-wise relationship. We note that  $T_{(i)}^*Q_{(i)} = T_{(i)}^* \text{diag}(w)T_{(i)}$ ,  $\forall(i)$  is a diagonal matrix. Hence we can write the following relationship between two frames:

$$T_{(i)}^*Q_{(i)}T_{(j)}^*z_{(j)} = T_{(i)}^*Q_{(i)}T_{(j)}^*Q_{(j)}\psi = T_{(j)}^*Q_{(j)}T_{(i)}^*Q_{(i)}\psi = T_{(j)}^*Q_{(j)}T_{(i)}^*z_{(i)},$$

i.e. the  $i$ -th frame multiplied by the  $j$ -th illumination is equal to the  $j$ -th frame multiplied by the  $i$ -th illumination, after putting the results back to the right position. In other words, we have a pairwise relationship

$$\sum_{i,j} \|T_{(j)}^*Q_{(j)}T_{(i)}^*z_{(i)} - T_{(i)}^*Q_{(i)}T_{(j)}^*z_{(j)}\| = 0. \quad (9)$$

By swapping diagonal matrices  $T_{(i)}^*Q_{(i)}$  and using  $T_{(i)}T_{(i)}^* = I$ , we can write out the pairwise discrepancy between all frames:

$$\frac{1}{2} \sum_{i,j} \|T_{(j)}^*Q_{(j)}T_{(i)}^*z_{(i)} - T_{(i)}^*Q_{(i)}T_{(j)}^*z_{(j)}\|^2 = \sum_{i,j} z_{(i)}^* \left[ \mathbb{Q}_{(i)}^2 \delta_{i,j} - Q_{(i)}Q_{(j)}^* \right] z_{(j)} = \mathbf{z}^*[\mathbb{Q}^2 - \mathbb{P}]\mathbf{z}$$

where  $\mathbb{Q}_{(i)}^2 \equiv T_{(i)}\mathbf{Q}^*\mathbf{Q}T_{(i)}^*$ ,  $\mathbb{Q}^2 \equiv \text{diag}(\mathbb{Q}_{(i=1\dots k)}^2)$ ,  $\mathbb{P} \equiv \mathbf{Q}\mathbf{Q}^*$ . Indeed, note that  $\sum_{i,j} z_{(i)}^* \mathbf{T}_{(i)}\mathbf{Q}_{(j)}^*\mathbf{Q}_{(j)}\mathbf{T}_{(i)}^*z_{(i)} = \sum_i z_{(i)}^* \mathbf{T}_{(i)} \left[ \sum_j \mathbf{Q}_{(j)}^* \mathbf{Q}_{(j)} \right] \mathbf{T}_{(i)}^*z_{(i)}$  and  $\mathbf{Q}^*\mathbf{Q} = \sum_j \mathbf{Q}_{(j)}^* \mathbf{Q}_{(j)}$ . Note that  $\mathbf{Q}^*\mathbf{Q}$  is a diagonal matrix with non-negative diagonal entries describing how a pixel of the object of interest is illuminated by different windows. Thus we can define  $\mathbb{Q}$  by taking square root of  $\mathbb{Q}^2$  entry-wisely. We may assume that the diagonal is positive, otherwise some information of the object is missed in the experiment. Thus we may define  $\mathbb{Q}^{-1}$ . Also note that by a direct calculation, we obtain

$$\mathbb{Q}^2 = \text{diag}(\mathbf{T}\mathbf{T}^*\mathbf{S}|w|^2). \quad (10)$$

Intuitively,  $\mathbf{T}^*\mathbf{S}|w|^2$  describes how pixels of the whole  $\psi$  is illuminated, and  $\mathbf{T}_{(i)}\mathbf{T}^*\mathbf{S}|w|^2$  is how the pixels of the  $i$ -th patch of  $\psi$  is illuminated, which is the same as  $T_{(i)}\mathbf{Q}^*\mathbf{Q}T_{(i)}^*$ .

We can minimize this functional by first renormalizing, making a change of variable  $\hat{\mathbf{z}} = \mathbb{Q}\mathbf{z}$ , then applying the power iteration:

$$\mathbf{z}^*[\mathbb{Q}^2 - \mathbb{P}]\mathbf{z} = \hat{\mathbf{z}}^*[I - \mathbb{Q}^{-1}\mathbb{P}\mathbb{Q}^{-1}]\hat{\mathbf{z}} = \hat{\mathbf{z}}^*[I - P_Q]\hat{\mathbf{z}} \quad (11)$$

$$\mathbf{z} \leftarrow \mathbb{Q}^{-1}P_Q\hat{\mathbf{z}} = \mathbb{Q}^{-1}P_Q\mathbb{Q}\mathbf{z} = P_Q\mathbf{z}, \quad (12)$$

which holds by the way  $\mathbb{Q}$  is defined. The reason for the above formulation is to establish a relationship between  $\mathbb{Q}$  and  $\mathbf{z}$ . As we have seen in Sec. II, the relationship between  $w$  and  $\psi$  in (Eq. (7)) is used to recover both  $w$  and  $\psi$ .

Interestingly, the relationship (Eq. 9) is symmetric w.r.t.  $Q$  (i.e.  $w$ ) and  $z$ . In other words, we can update the probe based on the frames  $z$  by solving the symmetric counterpart:

$$\begin{aligned} \frac{1}{2} \sum_{i,j} \|T_{(j)}^* Q_{(j)} T_{(i)}^* z_{(i)} - T_{(i)}^* Q_{(i)} T_{(j)}^* z_{(j)}\|^2 &= \mathbf{z}^* [\mathbb{Q}^2 - \mathbb{P}] \mathbf{z} = \mathbf{z}^* [\text{diag}(\mathbf{T}\mathbf{T}^* \mathbf{S} |w|^2) - \text{diag}(\mathbf{S}w) \mathbf{T}\mathbf{T}^* \text{diag}(\mathbf{S}\bar{w})] \mathbf{z} \\ &= w^* \mathbf{S}^* [\text{diag}(\mathbf{T}\mathbf{T}^* |z|^2) - \text{diag}(z) \mathbf{T}\mathbf{T}^* \text{diag}(\bar{z})] \mathbf{S}w, \end{aligned}$$

where the second equality holds due to (10) and (4), and the last equality holds due to the equality  $\mathbf{z}^* \text{diag}(\mathbf{T}\mathbf{T}^* \mathbf{S} |w|^2) \mathbf{z} = w^* \mathbf{S}^* \text{diag}(\mathbf{T}\mathbf{T}^* |z|^2) \mathbf{S}w$  by a direct calculation. Note that

1. we may view  $\mathbf{z}^* \text{diag}(\mathbf{T}\mathbf{T}^* \mathbf{S} |w|^2) \mathbf{z}$  as a weighted inner product in  $\mathbb{C}^{Km^2}$ ;
2. when  $z \in \mathbb{C}^{Km^2}$  is the vectorized version of all illuminated images, geometrically  $\mathbf{S}^* \text{diag}(z) \mathbf{S}$  means averaging over all illuminated images; that is  $\mathbf{S}^* \text{diag}(z) \mathbf{S} = \text{diag}(\sum_{i=1}^K z_{(i)})$ . By a directly calculation, we have  $\mathbf{S}^* \text{diag}(z) \mathbf{S} = \text{diag}(\mathbf{S}^* z)$ .

With the above preparation, we wish to solve:

$$\arg \min_w w^* \mathbf{S}^* [\text{diag}(\mathbf{T}\mathbf{T}^* |z|^2) - \text{diag}(\bar{z}^*) \mathbf{T}\mathbf{T}^* \text{diag}(\bar{z})] \mathbf{S}w, \quad (13)$$

which can be expressed as (in a similar form as Eq. (11))

$$\begin{aligned} \arg \min_w w^* [D - A]w, \quad (14) \\ \text{where } \begin{cases} D = \mathbf{S}^* \text{diag}(\mathbf{T}\mathbf{T}^* |z|^2) \mathbf{S} = \text{diag}(\mathbf{S}^* (\mathbf{T}\mathbf{T}^* |z|^2)) \\ A = \mathbf{S}^* [\text{diag}(\bar{z}^*) \mathbf{T}\mathbf{T}^* \text{diag}(\bar{z})] \mathbf{S}. \end{cases} \end{aligned}$$

Note that  $A$  is Hermitian but not a diagonal matrix since  $\text{diag}(\bar{z}^*) \mathbf{T}\mathbf{T}^* \text{diag}(\bar{z})$  is not diagonal. Thus, (14) yields - by power method, starting from an initial estimate  $w$ :

$$w \leftarrow D^{-1} A w = \frac{\mathbf{S}^* \text{diag}(\bar{z}^*) \mathbf{T}\mathbf{T}^* \text{diag}(\bar{z}) \mathbf{S}w}{\mathbf{S}^* \mathbf{T}\mathbf{T}^* |z|^2} = \frac{\mathbf{S}^* \text{diag}(z) \mathbf{T}\mathbf{T}^* \text{diag}(\mathbf{S}w) \bar{z}}{\mathbf{S}^* \mathbf{T}\mathbf{T}^* |z|^2} = \frac{\mathbf{S}^* \text{diag}(z) \mathbf{T} \mathbf{Q}^* \bar{z}}{\mathbf{S}^* \mathbf{T}\mathbf{T}^* |z|^2}, \quad (15)$$

where the last equality holds due to (4). Note the projection update (12) can be expressed in a similar way by swapping the order of  $\mathbf{S}$  with  $\mathbf{T}\mathbf{T}^*$ :

$$z \leftarrow P_{\mathbf{Q}} z = \frac{\mathbf{Q}\mathbf{Q}^* z}{\mathbf{Q}^2} = \frac{\text{diag}(\mathbf{S}w) \mathbf{T}\mathbf{T}^* \text{diag}(\mathbf{S}w)^* z}{\mathbf{T}\mathbf{T}^* \mathbf{S} |w|^2}.$$

How does this update relate to the standard update in (7) blue? If we insert  $\mathbb{Q}^2$  inside the averaging matrices  $\mathbf{S}^*(\cdot)\mathbf{S}$  and when  $z = \mathbf{Q}\psi$ , we obtain

$$w = \frac{\mathbf{S}^* \mathbb{Q}^{-2} \text{diag}(z) \mathbf{T}\mathbf{T}^* \text{diag}(\bar{z}) \mathbf{S}w}{\mathbf{S}^* \mathbb{Q}^{-2} \mathbf{T}\mathbf{T}^* |z|^2} = \frac{\mathbf{S}^* \text{diag}(z) \mathbf{T} \left[ \frac{1}{\mathbb{Q}^* \mathbb{Q}} \mathbf{T}^* \text{diag}(\bar{z}) \mathbf{S}w \right]}{\mathbf{S}^* \mathbf{T} \left[ \frac{1}{\mathbb{Q}^* \mathbb{Q}} \mathbf{T}^* |z|^2 \right]} = \frac{\mathbf{S}^* \text{diag}(\mathbf{T}\bar{\psi}) z}{\mathbf{S}^* \mathbf{T} |\psi'|^2},$$

where the third equality holds since  $\mathbf{T}^* \text{diag}(\bar{z}) \mathbf{S}w = \mathbf{T}^* \text{diag}(\mathbf{S}w) \bar{z} = \overline{\mathbf{T}^* \text{diag}(\mathbf{S}\bar{w}) z} = \overline{\mathbf{Q}^* z}$  and  $\psi = (\mathbf{Q}^* \mathbf{Q})^{-1} \mathbf{Q}^* z$ , and we define  $|\psi'|^2 \equiv \frac{1}{\mathbb{Q}^* \mathbb{Q}} \mathbf{T}^* |z|^2$ . Note that  $\frac{1}{\mathbb{Q}^* \mathbb{Q}} \mathbf{T}^* |z|^2$  is different from  $|\psi|^2 = \frac{1}{\mathbb{Q}^* \mathbb{Q}} \mathbf{Q}^* z|^2$  in (7). However  $\mathbf{S}^* \mathbf{T}$  in (15) smears out the normalization factor, and the two results are similar.

#### IV. RANK-1 SPEEDUP FOR WEAKLY SCATTERING AND PIECEWISE SMOOTH OBJECTS

A simple way to speed up is to simply remove one constant term (DC) on the fly, that is we compute the *transparency* factor  $\nu \in \mathbb{C}^1$  and subtract the average transmitted light: if we replace  $z \leftarrow z - \nu \mathbf{S}w$  in Eqs. (14, 15) we get the following update:

$$\nu = \frac{(\mathbf{S}w)^* \mathbf{z}}{\|\mathbf{S}w\|^2}, \quad w \leftarrow \frac{\mathbf{S}^* (\text{diag}(\mathbf{z} - \nu \mathbf{S}w) \mathbf{T} \bar{\mathbf{Q}}^* (\bar{\mathbf{z}} - \bar{\nu} \mathbf{S}w))}{\mathbf{S}^* (\mathbf{T} \mathbf{T}^* |\mathbf{z} - \nu \mathbf{S}w|^2)} = \frac{\mathbf{S}^* (\text{diag}(\mathbf{z} - \nu w) (\mathbf{T} \bar{\mathbf{Q}}^* \bar{\mathbf{z}} - \bar{\nu} \mathbf{Q}^2))}{\mathbf{S}^* (\mathbf{T} \mathbf{T}^* |\mathbf{z}|^2 - 2\Re(\bar{\nu} \mathbf{T} \mathbf{Q}^* \mathbf{z}) + \mathbf{Q}^2 |\nu|^2)}, \quad (16)$$

where the last equality holds by (10).

This is useful when an object has a strong DC term (weak contrast). Moreover, we can remove the frame-wise DC term for piecewise objects, which is useful since any constant region within the object does not provide any information about the probe. The second formulation enables us to compute  $\nu$  frame-wise.

We simply average the frames that overlap together, that is we apply the operator that sums all the frames that overlap with a given frame. Consider the  $K \times K$  matrix  $\mathbf{X}$ , with entries  $\mathbf{X}(i, j) = 1$  if  $(i)$  overlaps with  $(j)$ , or 0 otherwise. Compute the  $v \in \mathbb{C}^K$  vector:

$$v_i = \frac{\sum_j \mathbf{X}_{i,j} (w^* \mathbf{z}_{(j)})}{\sum_j \mathbf{X}_{i,j} (\|w\|^2)} = \frac{\sum_j \mathbf{X}_{i,j} (w^* \mathbf{z}_{(j)})}{\|w\|^2 \sum_j \mathbf{X}_{i,j}}$$

Then do the following update, which we write with some abuse of notation:

$$w \leftarrow \frac{\mathbf{S}^* (\text{diag}(\mathbf{z} - \nu \mathbf{S}w) (\mathbf{T} \bar{\mathbf{Q}}^* \bar{\mathbf{z}} - \bar{\nu} \mathbf{Q}^2))}{\mathbf{S}^* (\mathbf{T} \mathbf{T}^* |\mathbf{z}|^2 - 2\Re(\bar{\nu} \mathbf{T} \mathbf{Q}^* \mathbf{z}) + \mathbf{Q}^2 |\nu|^2)}$$

the abuse of notation is that  $(\mathbf{S}w)v$ ,  $\mathbf{Q}\bar{v}$  and others, are intended as  $(\mathbf{S}w)\mathbf{B}v$  where  $\mathbf{B}$  is the matrix that replicates  $v_i$  onto the frame of dimension  $n^2$ .

Numerical tests are shown in Fig. 2 with  $n = 223$ ,  $m = 128$ ,  $K = 20 \times 20$ , 5 pixels steps. Significant speedup is observed using the update in Eq. (16), vs Eq. (7), the speedup is accentuated when there is a strong average constant transmission factor.

## V. ACKNOWLEDGEMENTS

This work is partially supported by the Center for Applied Mathematics for Energy Research Applications (CAM-ERA), which is a partnership between Basic Energy Sciences (BES) and Advanced Scientific Computing Research (ASRC) at the U.S Department of Energy under contract DE-AC02-05CH11231 (SM).

<sup>1</sup> Brian Abbey, Keith A. Nugent, Garth J. Williams, Jesse N. Clark, Andrew G. Peele, Mark A. Pfeifer, Martin de Jonge, and Ian McNulty. Keyhole coherent diffractive imaging. *Nature Physics*, 4:394–398, 03 2008.

<sup>2</sup> D J Batey, D Claus, and J M Rodenburg. Information multiplexing in ptychography. *Ultramicroscopy*, 138:13–21, 2014.

<sup>3</sup> Mike Beckers, Tobias Senkbeil, Thomas Gorniak, Klaus Giewekemeyer, Tim Salditt, and Axel Rosenhahn. Drift correction in ptychographic diffractive imaging. *Ultramicroscopy*, 126(0):44–47, 2013.

<sup>4</sup> H. N. Chapman. Phase-retrieval x-ray microscopy by wigner -distribution deconvolution. *Ultramicroscopy*, 66:153–172, 1996.

<sup>5</sup> Siyuan Dong, Radhika Shiradkar, Pariksheet Nanda, and

Guoan Zheng. Spectral multiplexing and coherent-state decomposition in fourier ptychographic imaging. *Biomedical Optics Express*, 5(6):1757–1767, 2014.

<sup>6</sup> J. R. Fienup, J. C. Marron, T. J. Schulz, and J. H. Seldin. Hubble space telescope characterized by using phase-retrieval algorithms. *Appl. Opt.*, 32(10):1747–1767, Apr 1993.

<sup>7</sup> Pierre Godard, Marc Allain, Virginie Chamard, and John Rodenburg. Noise models for low counting rate coherent diffraction imaging. *Opt. Express*, 20(23):25914–25934, Nov 2012.

<sup>8</sup> M. Guizar-Sicairos and J. R. Fienup. Phase retrieval with transverse translation diversity: a nonlinear optimization approach. *Opt. Express*, 16:7264–7278, 2008.

<sup>9</sup> Manuel Guizar-Sicairos and James R. Fienup. Mea-

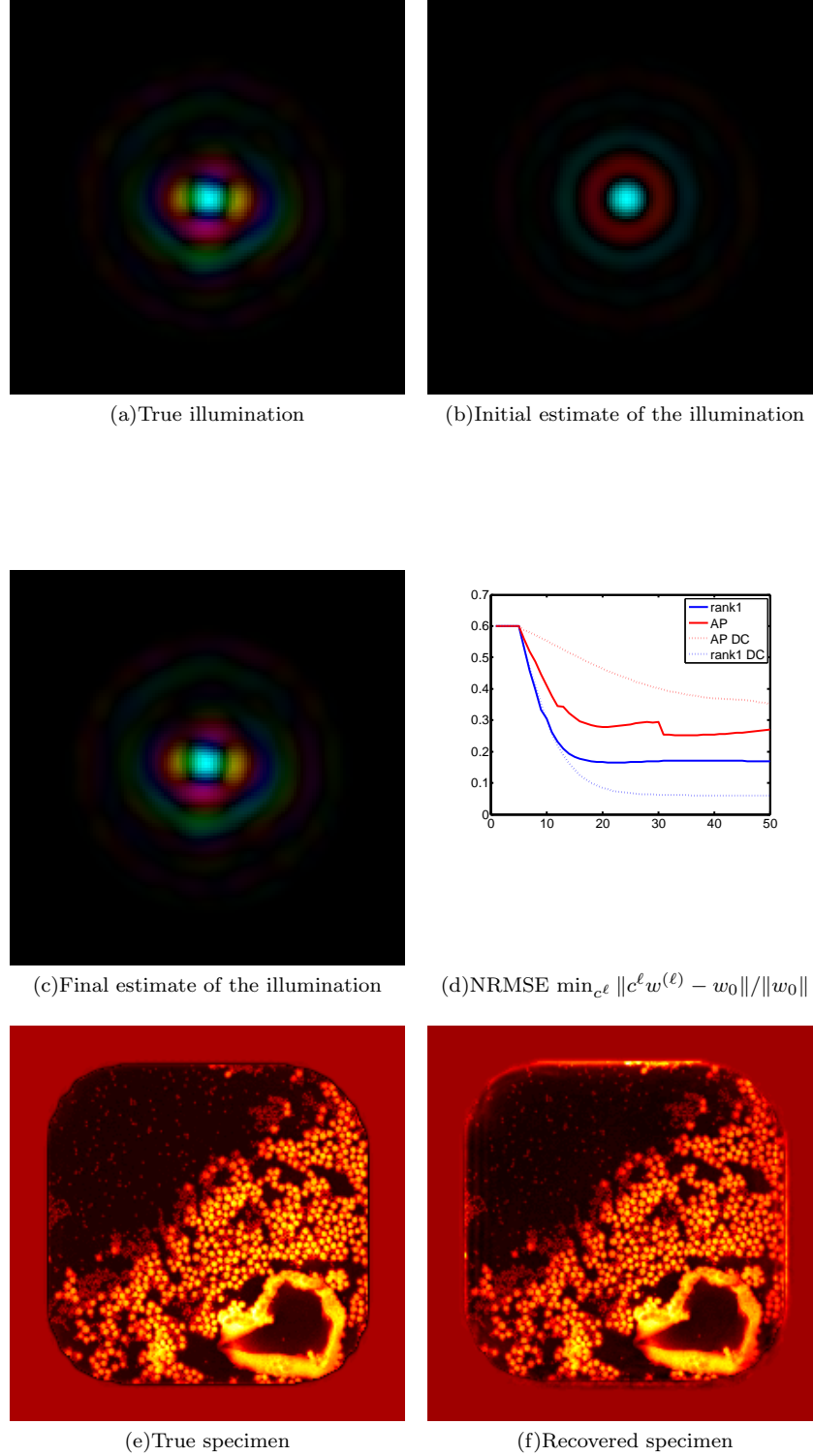


FIG. 2. Initial probe, true illumination, final illumination. Convergence with strong DC term (99%) or with DC term removed. test object, reconstruction. Residual disparities are ascribed to global translations between the “true” illumination and image used for simulations. At every illumination update, the center of mass of the illuminations is centered within one neighboring pixel. Further analysis of fractional shifts and aberrations can be performed using the prescription given in<sup>17</sup>.

- surement of coherent x-ray focusedbeams by phase retrieval with transversetranslation diversity. *Opt. Express*, 17(4):2670–2685, Feb 2009.
- <sup>10</sup> Manuel Guizar-Sicairos, Suresh Narayanan, Aaron Stein, Meredith Metzler, Alec R. Sandy, James R. Fienup, and Kenneth Evans-Lutterodt. Measurement of hard x-ray lens wavefront aberrations using phase retrieval. *Applied Physics Letters*, 98(11):111108, 2011.
  - <sup>11</sup> R. Hegerl and W. Hoppe. Dynamic theory of crystalline structure analysis by electron diffraction in inhomogeneous primary wave field. *Berichte Der Bunsen-Gesellschaft Fur Physikalische Chemie*, 74:1148, 1970.
  - <sup>12</sup> Susanne Höning, Robert Hoppe, Jens Patommel, Andreas Schropp, Sandra Stephan, Sebastian Schöder, Manfred Burghammer, and Christian G. Schroer. Full optical characterization of coherent x-ray nanobeams by ptychographic imaging. *Opt. Express*, 19(17):16324–16329, Aug 2011.
  - <sup>13</sup> W. Hoppe. Beugung im inhomogenen Primärstrahlwellenfeld. I. Prinzip einer Phasenmessung von Elektronenbeugungsinterferenzen. *Acta Crystallographica Section A*, 25(4):495–501, Jul 1969.
  - <sup>14</sup> N. C. Jesse and G. P. Andrew. Simultaneous sample and spatial coherence characterisation using diffractive imaging. *Applied Physics Letters*, 99(15):154103, 2011.
  - <sup>15</sup> C.M. Kewish, P. Thibault, M. Dierolf, O. Bunk, A. Menzel, J. Vila-Comamala, K. Jefimovs, and F. Pfeiffer. Ptychographic characterization of the wavefield in the focus of reflective hard x-ray optics. *Ultramicroscopy*, 110:325–9, Mar 2010.
  - <sup>16</sup> A.M. Maiden, M.J. Humphry, M.C. Sarahan, B. Kraus, and J.M. Rodenburg. An annealing algorithm to correct positioning errors in ptychography. *Ultramicroscopy*, 120(0):64 – 72, 2012.
  - <sup>17</sup> S Marchesini, HN Chapman, A Barty, C Cui, MR Howells, JCH Spence, U Weierstall, and AM Minor. Phase aberrations in diffraction microscopy. *IPAP Conf. Series 7 pp.380-382, 2006, arXiv preprint physics/0510033*, 2006.
  - <sup>18</sup> Stefano Marchesini, Andre Schirotzek, Chao Yang, Hautieng Wu, and Filipe Maia. Augmented projections for ptychographic imaging. *Inverse Problems*, 29(11):115009, 2013.
  - <sup>19</sup> Stefano Marchesini, Yu-Chao Tu, and Hau-tieng Wu. Alternating projection, ptychographic imaging and phase synchronization. *arXiv preprint arXiv:1402.0550*, 2014.
  - <sup>20</sup> Joanne Marrison, Lotta Rätty, Poppy Marriott, and Peter O’Toole. Ptychography—a label free, high-contrast imaging technique for live cells using quantitative phase information. *Scientific reports*, 3, 2013.
  - <sup>21</sup> Dustin B Moore and James R Fienup. Transverse translation diversity wavefront sensing with limited position and pupil illumination knowledge. In *SPIE Astronomical Telescopes+ Instrumentation*, pages 91434F–91434F. International Society for Optics and Photonics, 2014.
  - <sup>22</sup> J. M. Rodenburg and R. H. T. Bates. The theory of super-resolution electron microscopy via wigner-distribution deconvolution. *Phil. Trans. R. Soc. Lond. A*, 339:521–553, 1992.
  - <sup>23</sup> J. M. Rodenburg and H. M. L. Faulkner. A phase retrieval algorithm for shifting illumination. *Appl. Phys. Lett.*, 85:4795–4797, 2004.
  - <sup>24</sup> Andreas Schropp, Robert Hoppe, Vivienne Meier, Jens Patommel, Frank Seiboth, Hae Ja Lee, Bob Nagler, Eric C Galtier, Brice Arnold, Ulf Zastra, et al. Full spatial characterization of a nanofocused x-ray free-electron laser beam by ptychographic imaging. *Scientific reports*, 3, 2013.
  - <sup>25</sup> John CH Spence. *High-resolution electron microscopy*, volume 60. Clarendon Press, 2003.
  - <sup>26</sup> Marco Stockmar, Peter Cloetens, Irene Zanette, Björn Enders, Martin Dierolf, Franz Pfeiffer, and Pierre Thibault. Near-field ptychography: phase retrieval for in-line holography using a structured illumination. *Scientific reports*, 3, 2013.
  - <sup>27</sup> P. Thibault, M. Dierolf, O. Bunk, A. Menzel, and F. Pfeiffer. Probe retrieval in ptychographic coherent diffractive imaging. *Ultramicroscopy*, 109:338–43, Mar 2009.
  - <sup>28</sup> P. Thibault, M. Dierolf, A. Menzel, O. Bunk, C. David, and F. Pfeiffer. High-Resolution scanning x-ray diffraction microscopy. *Science*, 321(5887):379–382, 2008.
  - <sup>29</sup> P. Thibault and M. Guizar-Sicairos. Maximum-likelihood refinement for coherent diffractive imaging. *New Journal of Physics*, 14(6):063004, 2012.
  - <sup>30</sup> Samuel T Thurman and James R Fienup. Phase retrieval with signal bias. *JOSA A*, 26(4):1008–1014, 2009.
  - <sup>31</sup> Lei Tian, Xiao Li, Kannan Ramchandran, and Laura Waller. Multiplexed coded illumination for fourier ptychography with an led array microscope. *Biomedical Optics Express*, 5(7):2376–2389, 2014.
  - <sup>32</sup> DJ Vine, GJ Williams, B Abbey, MA Pfeifer, JN Clark, MD De Jonge, I McNulty, AG Peele, and KA Nugent. Ptychographic fresnel coherent diffractive imaging. *Physical Review A*, 80(6):063823, 2009.
  - <sup>33</sup> Z. Wen, C. Yang, X. Liu, and S. Marchesini. Alternating direction methods for classical and ptychographic phase retrieval. *Inverse Problems*, 28(11):115010, 2012.
  - <sup>34</sup> L. W. Whitehead, G. J. Williams, H. M. Quiney, D. J. Vine, R. A. Dilanian, S. Flewett, K. A. Nugent, A. G. Peele, E. Balaur, and I. McNulty. Diffractive imaging using partially coherent x rays. *Phys. Rev. Lett.*, 103:243902, Dec 2009.
  - <sup>35</sup> Antoine Wojdyla, Ryan Miyakawa, and Patrick Naulleau. Ptychographic wavefront sensor for high-na euv inspection and exposure tools. In *SPIE Advanced Lithography*, pages 904839–904839. International Society for Optics and Photonics, 2014.
  - <sup>36</sup> C. Yang, J. Qian, A. Schirotzek, F. Maia, and S. Marchesini. Iterative Algorithms for Ptychographic Phase Retrieval. *ArXiv e-prints*, May 2011.
  - <sup>37</sup> Guoan Zheng, Roarke Horstmeyer, and Changhui Yang. Wide-field, high-resolution fourier ptychographic microscopy. *Nature Photonics*, 7(9):739–745, 2013.